

1
2 **Title: An unexpected large continental source of reactive bromine and chlorine with**
3 **significant impact on wintertime air quality**

4
5 **Short Title: Coal burning is a large continental bromine source**

6
7 **Authors:** Xiang Peng^{1†}, Weihao Wang^{1†}, Men Xia¹, Hui Chen², A.R. Ravishankara³, Qinyi
8 Li⁴, Alfonso Saiz-Lopez⁴, Pengfei Liu⁵, Fei Zhang², Chenglong Zhang⁵, Likun Xue⁶, Xinfeng
9 Wang⁶, Christian George⁷, Jinhe Wang⁸, Yujing Mu⁵, Jianmin Chen², Tao Wang^{1*}

10 **Affiliations:**

11 ¹ Department of Civil and Environmental Engineering, the Hong Kong Polytechnic University,
12 Hong Kong, China.

13 ² Department of Environmental Science and Engineering, Fudan University, Institute of
14 Atmospheric Sciences, Shanghai, China.

15 ³ Departments of Atmospheric Science and Chemistry, Colorado State University, Fort Collins,
16 CO, USA

17 ⁴ Department of Atmospheric Chemistry and Climate, Institute of Physical Chemistry
18 Rocasolano, CSIC, Madrid 28006, Spain.

19 ⁵ Research Center for Eco-Environmental Sciences, Chinese Academy of Sciences, Beijing,
20 100085, China.

21 ⁶ Environment Research Institute, Shandong University, Qingdao, Shandong, China

22 ⁷ Univ Lyon, Université Claude Bernard Lyon 1, CNRS, IRCELYON, F-69626, Villeurbanne,
23 France.

24 ⁸ School of Municipal and Environmental Engineering, Shandong Jianzhu University, Jinan,
25 Shandong, China.

26 *Correspondence to Tao Wang (cetwang@polyu.edu.hk).

27 † These authors contributed equally to this work.

28
29 **ABSTRACT:**

30 Halogen atoms affect the budget of ozone and the fate of pollutants such as
31 hydrocarbons and mercury. Yet their sources and significances in polluted continental regions
32 are poorly understood. Here we report the observation of unprecedented levels (averaging to
33 hundreds of parts per trillion) of bromine chloride (BrCl) at a mid-latitude site in North China
34 during winter. Widespread coal burning in rural households and a photo-assisted process were
35 the main source of BrCl and other bromine gases. BrCl contributed about 55% of both bromine

36 (Br) and chlorine (Cl) atoms. The halogen atoms increased the abundance of 'conventional'
37 tropospheric oxidants (OH, HO₂, and RO₂) by 26-73%, and enhanced oxidation of hydrocarbon
38 by nearly a factor of two and the net ozone production by 55%. Our study reveals the significant
39 role of reactive halogen in winter atmospheric chemistry and in the deterioration of air quality
40 in continental regions where uncontrolled coal combustion is prevalent.

41 **Keywords:** BrCl, reactive halogen, oxidation, coal burning, air pollution, northern China

42 43 **MAIN TEXT**

44 45 **Introduction**

46 Halogen atoms (Cl and Br) can strongly influence the atmospheric chemical
47 composition. High levels of halogens have been shown to deplete ozone in the stratosphere [1]
48 and destroy ground level ozone of the Arctic [2-4]. There is an emerging recognition that in
49 the troposphere, they can kick start hydrocarbon oxidation that makes ozone, modify the
50 oxidative capacity by influencing the levels of OH and HO₂ radicals [5], perturb mercury
51 recycling by oxidizing elementary mercury (Hg⁰) to a highly toxic form (Hg^{II}) [4, 6]. Moreover,
52 Cl atoms can remove methane, a climate-forcing agent [7]. While most of the earlier halogen
53 studies focused on the stratosphere and the marine boundary layer, there has been growing
54 interest in the effect of Cl atoms on atmospheric chemistry over continental areas in the recent
55 decade because of the existence of anthropogenic chloride sources which can be activated to
56 form Cl atoms [8, 9]. Most of the previous studies focused on two Cl precursors, ClNO₂ and
57 Cl₂ [10-13], which were found to enhance ozone formation via Cl oxidation of hydrocarbons
58 [14-16]. However, little is known about the abundance and the role of bromine compounds in
59 the polluted continental troposphere. During a recent winter field study in the North China
60 Plain (NCP), we observed surprisingly high levels of bromine chloride (BrCl), which provides
61 a new and significant source of Br and Cl atoms. We show that intense coal burning and
62 photochemical reactions are responsible for the observed BrCl and other reactive bromine
63 gases. Through model simulations, we reveal that BrCl and other halogens may alter ozone
64 production, hydrocarbon oxidation, and conversion of elemental mercury to a soluble form in
65 the surface layer of the atmosphere of the highly polluted NCP.

66 67 **Results and Discussions**

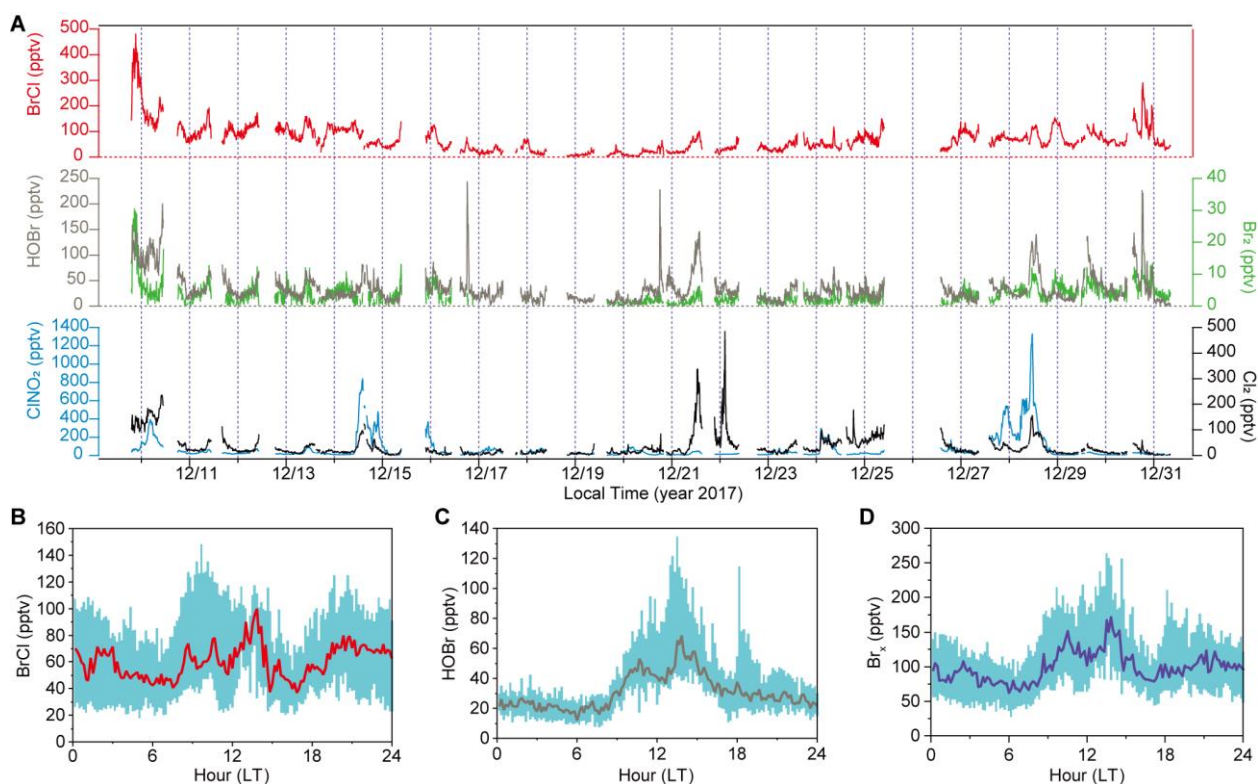
68 **Reactive halogen species observations**

69 Our measurements were conducted at the SRE-CAS station [17] in an agricultural field
70 in Hebei Province in the NCP during 9-31 December 2017 (Fig. S1A). The NCP is one of the
71 most populated regions in China and frequently suffers from severe haze pollution during
72 winter [18, 19] due to the high densities of human populations and industrial and agricultural
73 activities. Numerous villages are distributed in the NCP within distances of a few kilometers
74 between them (Fig. S1). The measurement site is surrounded by villages with residents of ~
75 1000, 1-2 km away from a national highway (G4) and 3-4 km away from a provincial road

76 (S335), and about 10 km southeast to Wangdu township (Fig. S1). During the field
77 measurement, the site was strongly impacted by emissions from road traffic and rural
78 household coal burning for heating and cooking. As the result, extremely high levels of NO_x
79 (83 ppbv on average) were observed with elevated SO_2 (14 ppbv on average) and $\text{PM}_{2.5}$ (137
80 $\mu\text{g}/\text{m}^3$ on average). The O_3 concentrations were low due to strong titration by high NO (53
81 ppbv on average) (Fig. S2 and S3).

82 Reactive halogen species (RHS), including BrCl , Cl_2 , ClNO_2 , Br_2 , and HOBr , were
83 measured using state-of-the-art chemical ionization mass spectrometry (CIMS) technique (see
84 Methods), which provided the first comprehensive measurement of RHS in China. The data
85 reveal three salient features. First, BrCl , a highly photolabile species, frequently exceeded 100
86 pptv with a maximum value of 482 pptv (10-min average) (Fig. 1A), which is more than 10
87 times larger than the previously reported highest value of 35 pptv in the Arctic [2] and 5 times
88 larger than the airborne measured value (80 pptv) during a 15-second transect of the exhaust
89 of a coal-fired power plant in the northeastern US [20]. Apart from these, BrCl had not been
90 detected in field studies outside of the polar regions [5]. Second, the average HOBr mixing
91 ratio (34 pptv) is also one order of magnitude larger than the level observed in the Arctic [21].
92 Third, BrCl and HOBr exhibited higher concentrations in the daytime (8:00-16:00) (local time,
93 LT), but with a considerable amount (~ 20 pptv) present at night (Fig. 1B, 1C). In terms of other
94 RHS, ClNO_2 concentrations were lower than the previously observed values in the same area
95 (but at a different location) in summer 2014 [14], while the levels of Cl_2 (Fig. 1A) were
96 comparable to the summer values [16]. Br_2 was present at very low levels with an average
97 mixing ratio of 4 ppt, which was 3 times lower than a recently reported value in the Arctic [4]
98 (Fig. 1A). Additional information on the measurement site and ancillary measurements are
99 given in the Method Section and Supplementary Materials Section 1 and Section 2.

100



101

102 **Fig. 1. Ambient surface mixing ratios and diurnal profiles of reactive halogen gases at a**
 103 **rural site in NCP during 9-31 December 2017. (A)** Time series of Cl_2 , ClNO_2 , HOBr , Br_2 ,
 104 and BrCl . **(B)** The diurnal profiles of BrCl for the entire period. The red line is the median, and
 105 the cyan shade represents the 25 percentile and 75 percentile value. **(C)** The diurnal profiles of
 106 HOBr for the entire period. The brown line is the median, and the cyan shade represents the 25
 107 percentile and 75 percentile value. **(D)** The diurnal profiles of gas-phase bromine Br_x ($= \text{BrCl}$
 108 $+ \text{HOBr} + 2 \times \text{Br}_2$) for the entire period. The purple line is the median, and the cyan shade
 109 represents the 25 percentile and 75 percentile value.

110

111

112 The source of reactive bromine species

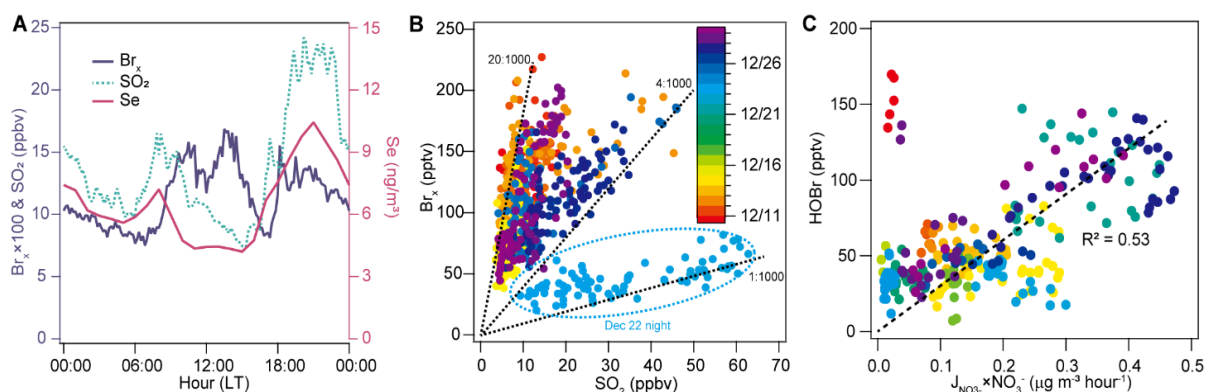
113 There is strong evidence that coal burning was a major source of the measured reactive
 114 bromine gases, Br_x , ($\text{Br}_x = \text{BrCl} + \text{HOBr} + 2 \times \text{Br}_2$). Br_x and two coal-burning tracers, sulfur
 115 dioxide (SO_2) and selenium (Se), all exhibited elevated levels in the morning and early evening
 116 (Fig. 2A), which is consistent with the increased coal use during these periods in rural homes
 117 for heating and cooking. Apart from emissions, the concentrations of the measured chemical
 118 species were also affected by the diurnal changes in the planetary boundary layer height
 119 (PBLH), which was not measured during the study period. The PBLH typically is at the
 120 maximum in the afternoon and reaches the minimum at night, which means that surface emitted
 121 pollutants are expected to experience maximum dilution during daytime and subject to the
 122 smallest dilution at night. Therefore, the morning increase in mixing ratios of Br_x , the coal
 123 burning tracers, and PBLH signify strong emission of local coal burning, whereas their later
 124 larger increase in levels was partly due to decreasing PBLH after sunset. Moreover, the Br_x
 125 showed a good positive correlation with SO_2 (Fig. 2B; R^2 of 0.56 ± 0.17) and Se (Fig. S4A; R^2
 126 of 0.58 ± 0.26) during the period of intensive coal burning (18:00-09:00) and when air masses

127 were relatively stable (wind speed <3 m/s and no abrupt change in temperature and relative
128 humidity). In addition, particulate halides (chloride and bromide) exhibited the morning and
129 early evening peaks (Fig. S3, A and B) and also correlated with SO₂ and Se (Fig. S4, B and C)
130 throughout the campaign, strongly indicating that coal burning was a substantial source of both
131 reactive bromine gaseous (Br_x) and particle halides observed at our site.

132 Fig. 2B and Fig. S4A indicate large variations in the observed ratios of Br_x to SO₂ or
133 Se, which can be explained by their relative content in coal, combustion conditions, and
134 atmospheric processing after emission. The unusual case on 22 December showed relatively
135 low levels of Br_x (~50 ppt) but very high loading of SO₂ (up to 80 ppb), resulting in the lowest
136 Br_x/SO₂ (1:1000, mole/mole, see Fig. 2B). The very high concentrations of trace metal elements
137 (Mn and Fe) in this case (Fig. S5) reveal that the air mass might be strongly impacted by
138 emissions from coal burning and ore processing in steel industries. The lowest Br_x/SO₂ ratios
139 may indicate a smaller emission of bromine relative to sulfur in iron-smelting processes,
140 incomplete activation of bromine in the air mass, or only partial accounting of reactive bromine
141 gases in the measured Br_x and more Br_x deposited relative to SO₂ in more aged air from the
142 steel factories (the nearest one is 80 km from the site). In comparison, the highest Br_x mixing
143 ratio was observed during the evening (19:00-24:00) on 9 December (Fig. 1A and Fig. S6) and
144 had a much larger Br_x/SO₂ ratio (13:1000, mole/mole), and this and most of the other cases
145 with moderate to high Br_x/SO₂ (4:1000-20:1000) in Fig. 2B could be characteristic of rural coal
146 burning.

147 There was no report on concurrent Br_x and S measurement in domestic coal burned
148 effluent in China, and also no previous studies concurrently measured Br, Cl, and S content in
149 Chinese coal. It is, therefore, difficult to link our observed Br_x/S ratio to that ratio in coals.
150 Nonetheless, we compared the ambient molar ratio of (Br_x+Br_{particle}) to (SO₂+S_{particle}) and
151 (Cl_x+Cl_{particle})/(SO₂+S_{particle}) with the average and range of Br/S [22, 23] and Cl/S [22, 24]
152 estimated from the reported contents in Chinese coals (see Supplementary Materials Section
153 4). We found that the ambient ratios were nearly one magnitude higher than the value of Br/S
154 and Cl/S in Chinese coal, suggesting that halogen compounds are released in much larger
155 proportion compared to sulfur, or there are other sulfur species like COS which are released
156 during the smoldering phase of coal burning but are not measured [25]. The Br_x/SO₂ ratios
157 observed in our study are one to two orders of magnitude higher than the ratio measured in the
158 northeastern US in the exhausts of coal-fired power plants that are not equipped with wet flue
159 gas desulfurization [20]. This result indicates that large amounts of reactive bromine species
160 could be released from rural domestic coal burning in the NCP region. Based on the average
161 content of Br and Cl in 137 representative Chinese coal samples [22] and the annual coal
162 assumption in the NCP, we estimate that the amount of Br and Cl in coal can account for our
163 observed atmospheric values (see Supplementary Materials Section 5).

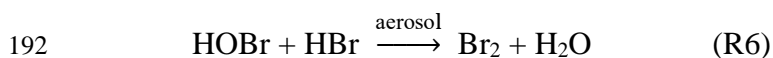
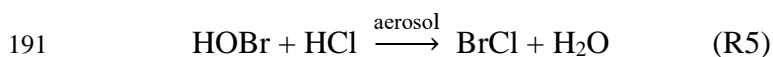
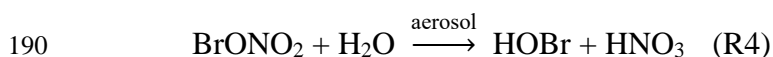
164



165

166 **Fig. 2. Evidence for the source of the observed reactive bromine gases: coal burning and**
 167 **photo-assisted activation process.** (A) Average diurnal profile of Br_x (purple line in 10-min
 168 average), SO₂ (green dash line in 10-min average), and Se (red line in 1-hour average) during
 169 9-31 December 2017. The lag in Br_x and its daytime peak are due to the photochemical release
 170 of Br_x from particulate matter. (B) Scatter plot of 10-min average Br_x and SO₂ from 18:00 to
 171 09:00 when the air masses are stable. Color coded according to sampling date on 9-31
 172 December 2017. (Br_x = BrCl + HOBr + 2×Br₂). The dotted lines indicate Br_x/SO₂ slope
 173 (mole/mole) of 1:1000 and 20:1000, which is the range of Br_x production from coal burning.
 174 Data in the oval depicts a case of industrial emissions. (C) Scatter plot of 10-min average HOBr
 175 and a proxy of photolysis rate of nitrate (J_{NO₃} × NO₃⁻ concentration) from 10:00 to 15:00. J_{NO₃}
 176 was calculated from the TUV model
 177 (http://cprm.acom.ucar.edu/Models/TUV/Interactive_TUV) under clear sky condition and then
 178 scaled to the measured J_{NO₂}. Color coded according to sampling date on 9-31 December 2017.
 179

180 Fig. 2A shows that the Br_x (and BrCl (Fig. 1B)) mixing ratios were highest in the
 181 afternoon and exhibited a larger fractional increase than SO₂. Considering that BrCl is rapidly
 182 photolyzed (the noon-time photolytic lifetime of ~4 minutes) and the PBLH increases during
 183 the daytime, the increase in Br_x mixing ratio reveals a significant additional source facilitated
 184 by sunlight in order to sustain the observed Br_x levels of in the daytime. The main
 185 photochemical chain cycle, which has been proposed to explain the elevated daytime Br_x in the
 186 Polar regions, involves R1-R8 [26].



195 The heterogeneous reaction of HOBr with HCl (R5) and with HBr (R6), which occurs
196 on the surfaces of snow, sea-salt aerosols, or frost flowers, is thought to be the main source for
197 the photolabile BrCl and Br₂, respectively [2, 5]. In the daytime, Br atom from photolysis of
198 Br₂ and BrCl initiates the above chain reactions to liberate more halogens from the condensed
199 phase, leading to a rapid increase in reactive bromine gases in daytime (“bromine explosion”)
200 [27].

201 In our study, the presence of elevated daytime BrCl and its good correlation of HOBr
202 loss rate (Fig. S7) suggests that R(5) plays an important role at our site, whereas the low Br₂
203 concentrations indicate less importance of R(6). The preference of R(5) to R(6) at our site may
204 be due to a much higher concentration of particulate chloride (7.3 μg/m³ on average) than that
205 of particulate bromide (0.07 μg/m³ on average). Because reaction R(5) only activates particulate
206 chloride (not bromide), the presently known bromine activation and propagation reactions (R1-
207 R8) cannot explain the increasing Br_x concentrations in the daytime, and there should be an
208 additional bromide activation process that produces HOBr or BrCl at our site. Previous
209 laboratory studies [28-30] observed production of Br₂ and BrCl when nitrate and halide in ice
210 or snow are illuminated with ultra-violet light, and it was hypothesized that photolysis of nitrate
211 aerosol generates OH radicals, which subsequently activate bromide to produce Br₂ and BrCl.
212 Pratt and co-workers [31] proposed another photochemical activation mechanism involving
213 nitrate, HCHO, H₂O₂, and O₃ based on an outdoor snow chamber experiment in the Arctic.
214 During our study, we found a moderate correlation between HOBr and the indicator of
215 photolysis rates of aerosol nitrate (the product of calculated J_{NO₃} and the measured PM_{2.5} nitrate
216 concentrations) during 10:00-15:00 (R²=0.53) (Fig. 2C), which suggests that the photolysis of
217 nitrate laden in particles may be involved in the activation of the bromide to produce HOBr
218 (and further BrCl). However, given the considerable scattering in the data, additional chemical
219 or physical processes may contribute to Br_x production, such as activation of bromide by an
220 organic photosensitizer [32].

221

222 **Significant impact on atmospheric chemistry**

223 Given the high reactivity of Cl and Br atoms, we calculate the impact of the high BrCl
224 and other photolabile Cl₂, Br₂, and ClNO₂ by using a photochemical box model that includes
225 up-to-date Cl and Br chemistry and by constraining the model with the relevant observation
226 data (see Supplementary Material Section 6). Photolysis of BrCl was the dominant source of
227 the Cl atoms (~56%), which was 14 times higher than the contribution from ClNO₂ and two
228 times larger than that from Cl₂ (Fig. S8A). The model predicted that Cl atoms reached a
229 maximum concentration of about ~9×10⁴ cm⁻³ at noon (Fig. 3B), and the average concentration
230 (1.6×10⁴ cm⁻³) is 26 times higher than the previously modeled global mean level of 620 cm⁻³
231 [33]. The peak Cl production rate at our site (~8×10⁶ cm⁻³s⁻¹, Fig. S8A) is more than 10 times
232 of that from photolysis of Cl₂ and ClNO₂ measured in early winter at a ground site near the
233 City of Manchester (UK) [12] and is several times of the primary Cl production rate from
234 ClNO₂ (predominantly) and Cl₂ observed during an aircraft campaign in the marine boundary
235 layer off the coast of New York City (US) in late winter [13]. The BrCl was also the dominant
236 source Br (~55%) at our site, followed by Br₂ (~20%) and BrO (~13%) (Fig. S8B). The
237 maximum Br production rate was 1.0×10⁷ cm⁻³s⁻¹ (Fig. S8B), which is two orders of magnitude

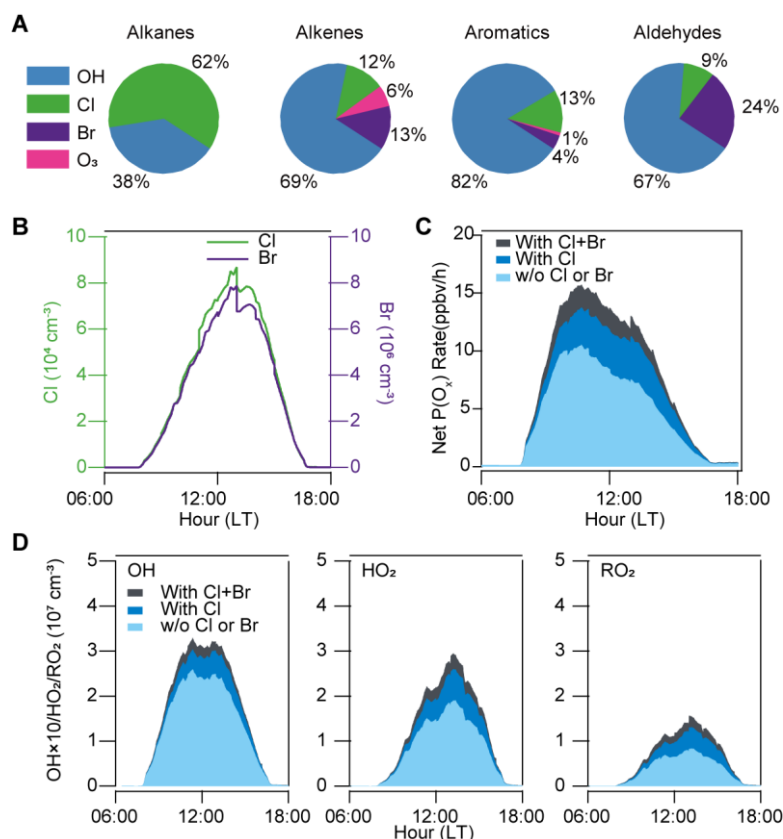
238 larger than the maximum Br production rate predicted without anthropogenic Br source in
239 polluted coastal areas in the wintertime [34].

240 We find that the high levels of Cl and Br atoms have a profound impact on the oxidation
241 of VOCs. On average, ~60% of alkanes, ~10% of alkenes, ~15% of aromatics, ~10% of
242 aldehyde was oxidized by Cl atoms during daytime (Fig. 3A) at the observation site. The Br
243 atoms contributed up to ~15% of alkenes and ~25% of aldehydes oxidation but negligibly to
244 the alkanes and aromatics (Fig. 3A) since Br reactions with these chemicals are very slow. The
245 reactions of VOCs with Cl and Br atoms produce RO₂ radicals, which are then recycled to form
246 HO₂ and OH radicals, increasing the average concentration of OH, HO₂, RO₂ oxidant radicals
247 by ~25%, ~50%, and ~75%, respectively (Fig. 3D). These results indicate that the abundance
248 (and impact) of HO_x radicals (OH, HO₂, and RO₂) would be significantly under-predicted if
249 the halogen species found in our study are not considered. A recent field measurement at a rural
250 site north of Beijing in January 2016 [35] has shown more than a factor of 1.5, 4, and 5 under-
251 predictions of OH, HO₂ and RO₂ under high NO_x condition when compared to the current
252 photochemical mechanism. The halogen (BrCl and Cl₂) induced chemistry could be part of the
253 reason for the under-estimation of HO_x.

254 When both direct (by halogen atoms) and indirect (from HO_x produced by the halogen
255 atom reactions) oxidation processes are included, the total VOCs oxidation rate increased by
256 ~180% for alkanes, ~50% for C₂-C₆ alkenes, ~40% for aromatics, and ~90% for aldehyde.
257 Moreover, the enhanced HO₂ and RO₂ increased O₃ production through reaction with NO. The
258 Cl and Br atoms enhanced the in-situ net chemical production rate of O_x (=O₃ + NO₂) (see
259 Supplementary Material Section 6) by 55% despite destroying ozone at the same time (Fig.
260 3C). Within these increases, Br atoms enhanced ~10% for OH, ~15% for HO₂, ~20% for RO₂,
261 and ~20% for net O_x production rate (Fig. 3, C and D). The result indicates that unlike the polar
262 and marine environments with low hydrocarbons, the Br atoms in the presence of hydrocarbons
263 can increase ozone production in polluted continental regions due to more abundant aldehyde
264 relative to O₃.

265 The halogen-initiated chemistry can also enhance secondary aerosol formation from
266 oxidations of VOCs. Since the oxidation of VOCs by radicals leads to SOA formation via
267 further reactions of RO₂ as well as other reactions with OH to form low-volatility molecules,
268 the halogen atoms, which has been shown to increase the RO₂ abundance by 75% on average,
269 will significantly increase SOA production. In addition, the halogen enhanced HO_x can
270 increase the production of other secondary aerosol observed during the haze events such as
271 sulfate (by boosting SO₂ oxidation with enhanced OH, O₃, and H₂O₂) and nitrate (via increasing
272 NO_x oxidation by OH and O₃ to form nitric acid). Therefore, the inclusion of halogen sources
273 discovered in our study in chemistry-transport models is likely to predict better the extent of
274 winter haze formation in North China.

275



276

277 **Fig. 3. The model calculated VOCs oxidation rates and radical abundance averaged for**
 278 **the entire period. (A) Relative contribution to the oxidation rates of alkanes, alkenes,**
 279 **aromatics, and aldehydes by OH, Cl, Br, and O₃. (B) The average diurnal profiles of Cl (green**
 280 **line) and Br (purple line) atoms. (C) The average diurnal profiles of net production rate of O_x**
 281 **(different color bars). The light blue bar, blue bar, and black bar represent results without Cl**
 282 **and Br chemistry, with only Cl chemistry, and with Cl and Br chemistry, respectively. (D) The**
 283 **average diurnal profiles of OH, HO₂, and RO₂. The light blue, blue, and black bars represent**
 284 **the same meaning as panel (C).**

285

286 The large abundance of Br atoms can also significantly increase the conversion of
 287 airborne elemental mercury (Hg⁰) to reactive mercury (Hg^{II}). Hg^{II} is more soluble and hence
 288 more prone to deposition to the surface than Hg⁰ and is the main mercury species that deposits
 289 and enter ecosystems. Therefore, enhancing atmospheric oxidation would increase mercury
 290 deposition to the environment near the source. At our site, the atmospheric lifetime of Hg⁰ due
 291 to oxidation by OH or Cl is estimated to be larger than 70 days, but it is shortened to only about
 292 2 days with the average Br atom concentration of 1.5×10⁶ cm⁻³ observed during the field study,
 293 which is much shorter than the global mercury lifetime of 10 to 13 months [36]. Given that
 294 coal burning also co-emits a large quantity of mercury [37] and the NCP has one of the highest
 295 surface concentrations of Hg⁰ in the world [36], the fast bromine-induced Hg^{II} formation and
 296 subsequent deposition may significantly increase the risk for human health and surface
 297 ecosystems in the NCP. Future studies are needed to extend our near-field measurements and
 298 modeling impact of halogens to the other parts of the boundary layer and downwind regions.

300 **Long-term and broad implications**

301 Although the above results are based on observations from one site, we believe that
302 these findings apply to a large portion of China, which utilizes coal burning to heat homes,
303 especially in rural areas. In the year 2017, 17 million households in Hebei province use coal as
304 one of their energy sources. The four provinces (Hebei, Shandong, Shanxi, and Henan) and
305 two municipalities (Beijing and Tianjin) in the NCP are projected by the China government to
306 account for 30% of China's total coal consumption in the year 2020 [38]. Therefore, BrCl is
307 expected to be ubiquitous over large areas of China with heavy coal burning, which is supported
308 by the observation of elevated levels of Br_x (up to 194 pptv) in March 2018 at the summit of
309 Mt. Tai, ~300 km south of the present site (Fig. S9).

310 Recognizing a large contribution to air pollution by rural coal burning, the Chinese
311 government embarked on a massive campaign since the winter of 2018 to replace low-quality
312 coal with natural gas and electricity in rural areas of North China [39]. A recent report [40]
313 finds that while some progress has been made, largely in Beijing's surrounding regions, the
314 conversion campaign has been challenging in north-western (Shaanxi and Shanxi) and north-
315 eastern China (Heilongjiang) due to insufficient natural gas supply, inadequate electricity
316 power grid, and the high costs of cleaner energy. Even within the NCP, the domestic coal
317 burning in the jurisdictions of Beijing, Tianjin and 26 other cities still accounted for about 40%
318 and 35% of the total emission of SO₂ and PM_{2.5} in the winter of 2019, with coal-fired electricity
319 and heat production and other industrial coal burning also contributing significantly [41]. The
320 plunge in the air quality in the middle of February 2020 in the NCP despite drastic reductions
321 in traffic and some industrial activities amid the Coronavirus epidemic and the Chinese New
322 Year holiday [41] signified the persistence of coal-burning induced air pollution. Therefore,
323 coal burning will likely be a long-lasting and important source of winter air pollution. Our
324 study demonstrates that the intense coal burning not only emits large amounts of primary
325 pollutants such as particulate and sulphur [42, 43], but also promote the formation of secondary
326 pollutants such as ozone, mercury (Hg^{II}), and organic aerosols by releasing highly reactive
327 halogen gases. The finding provides new scientific evidence to strengthen the impetus to
328 replace the use of dirty coal.

329 We note that as domestic coal burning is not limited to China, it is likely that similar
330 production of halogens occurs in other places where uncontrolled domestic coal burning is
331 common. According to the International Energy Agency, coal production in 2017 accounts for
332 27.1% of the world's total energy supply [44], and the top 20 coal consuming
333 countries/economies are distributed over all human-inhabited continents (Table. S1). The
334 dominant use of coal in developed countries such as the United States, Japan, and Germany is
335 for electricity generation, and stringent pollution control measures are generally utilized in
336 these countries. However, a larger proportion of coal use for non-electricity production [44]
337 and/or lower implementation of pollution control in other countries/economies make coal
338 burning as an important source of air pollutants not only in China, but possibly also in India,
339 Russia, and South Africa, etc. Previous source apportionment of ambient PM_{2.5} [45] and
340 bottom-up emission inventories [9] have indicated that coal burning is a major source of
341 atmospheric chloride, and field measurements in China and the US have observed elevated

364 nitrate, activate particulate Br to produce HOBr and BrCl. BrCl is also formed by the reaction
365 of HOBr with particulate Cl during day and night. BrCl is photolyzed to Cl and Br atoms in
366 the daytime. VOCs are oxidized by Cl atoms (mainly on alkanes) and Br atoms (mainly on
367 aldehydes) to produce ozone and secondary aerosols. Moreover, Br atoms significantly
368 accelerate the mercury deposition near the source. The potential formation of ClNO₂ is not
369 shown here. The background photo shows the nearby village and the location of the
370 measurement site. (Photo Credit: Chenglong Zhang and Pengfei Liu; RCEES, CAS).

371 METHODS

372 Field Measurements

373 Reactive halogen gases (RHS, including BrCl, HOBr, Br₂, Cl₂, ClNO₂, and N₂O₅), other
374 trace gases (HONO, H₂O₂, SO₂, CO, NO, NO₂, and O₃), aerosol concentration and
375 compositions, particle size distributions, VOCs, OVOCs, JNO₂, and other meteorological
376 parameters were simultaneously measured in this study. In this section, we describe in detail
377 the RHS measurements and present information for other measurements in the supplementary
378 materials.

379 A quadrupole chemical ionization mass spectrometer (Q-CIMS) (THS Instruments
380 LLC, Atlanta GA.) was used to measure BrCl, HOBr, Br₂, Cl₂, ClNO₂, and N₂O₅ by using
381 Iodide (I⁻) as a reagent ion. It had been used to measure N₂O₅ and ClNO₂ in previous studies
382 [14, 15]. In this study, each target species was monitored at more than two isotopic masses to
383 ensure accurate identifications of ion clusters. BrCl was monitored at 241 amu (I⁷⁹Br³⁵Cl⁻), 243
384 amu (I⁷⁹Br³⁷Cl⁻; I⁸¹Br³⁵Cl⁻) and 245 amu (I⁸¹Br³⁷Cl⁻). HOBr was monitored at 223 amu
385 (IHO⁷⁹Br⁻) and 225 amu (IHO⁸¹Br⁻). Br₂ was monitored at 287 amu (I⁷⁹Br⁸¹Br⁻) and 289 amu
386 (I⁸¹Br⁸¹Br⁻). Cl₂ was monitored at 197 amu (I³⁵Cl³⁵Cl⁻) and 199 amu (I³⁵Cl³⁷Cl⁻). ClNO₂ was
387 monitored at 208 amu (I³⁵ClNO₂⁻) and 210 amu (I³⁷ClNO₂⁻).

388 The CIMS instrument was housed in a single-story shelter. The sample line was a total
389 3.5 m long PFA-Teflon tubing (1/4 in. outer diameter), with the sampling inlet approximately
390 1.5 m above the rooftop. We tried to minimize potential inlet artifacts by (1) configuring the
391 sampling inlet system (Fig. S10) to divert large particles from the sample inlet into a by-pass
392 flow and reducing the residence time of the measured gases below 0.5 seconds; (2) changing
393 and washing the entire sampling inlet every day to reduce the deposition of Cl⁻ and Br⁻
394 containing particles on the inlet wall. There were no noticeable changes in the HOBr and BrCl
395 signals between before and after the tubing replacement (Fig. S11, B and C), strongly
396 suggesting that no significant heterogeneous reactions in the sample line after one-day use.

397 The instrument background signal was measured by scrubbing ambient air with alkaline
398 glass wool and charcoal, as many inorganic halogens are efficiently removed by this process,
399 which has also been used by other groups for halogen measurements [3, 16, 47]. The instrument
400 sensitivity for Cl₂ and ClNO₂ was determined on-site every two days. A Cl₂ permeation tube
401 was used as the calibration source, and its permeation rate (378 ng/min, variation <5%) was
402 determined before and after the campaign. The sensitivity of Cl₂ was stable (2.0±0.16 Hz/pptv)
403 (Fig. S12A) with no significant dependence on RH (Fig. S12B). The uncertainty for the Cl₂
404 measurement was about 25%. The calibration method of ClNO₂ has been reported in our
405 previous studies [14, 15]. The sensitivities for other halogen species (Br₂, HOBr, and BrCl)
406 were determined according to their sensitivity ratio relative to Cl₂ which was determined after
407 the field study. The calibration of Br₂ was similar to Cl₂, which was achieved by a permeation
408 tube standard. The HOBr was calibrated using the same method described by Liao et al. [3].
409 HOBr was synthesized from the reaction of liquid Br₂ with a 0.1 M silver nitrate solution
410 (AgNO₃), and its concentration was calculated from the Br₂ formation by passing the HOBr
411 standard through sodium bromide slurry (NaBr). The calibration of BrCl was achieved using
412 the method described by Neuman et al. [48], which was also used by Liao et al. [3] and Le
413 Breton et al. [49]. Briefly, the Br₂ and Cl₂ permeation tubes were placed in the same oven at
414 40 °C to produce BrCl via reaction of Cl₂+Br₂→2BrCl. We have confirmed in the laboratory

415 that all reduction of Br₂ and Cl₂ were converted into BrCl. The concentration of BrCl was
416 calculated from the reduction of Br₂. The sensitivity of Br₂, BrCl, and HOBr was 1.4 Hz/ppmv,
417 1.6 Hz/ppmv, and 2.1 Hz/ppmv, respectively. The measurement uncertainty for Br₂, BrCl, and
418 HOBr was about 25%, 35%, and 39%, respectively.

419 To make sure no significant spectral interference for signals of BrCl, HOBr, and Cl₂,
420 we checked their isotopic signals which showed strong correlation with slopes being close to
421 the respective theoretical isotopic ratio (Fig.S13). Potential artifacts from the inlet or
422 instrument are of critical concern. We have scrutinized all key steps in our CIMS measurements
423 and made sure that the HOBr and BrCl measurements did not suffer significant artifacts. We
424 examined five potential artifacts in the inlet or instrument: (i) Inlet artifacts from O₃
425 heterogeneous reactions, (ii) Potential secondary ion chemistry with IO₃⁻ in the ion chamber.
426 (iii) Secondary ion chemistry with IH₂O⁻ in the ion chamber. (iv) Mass spectral influence from
427 SO₂. (v) Inlet artifacts for BrCl measurement from further HOBr reactions. The detailed results
428 are provided in SI. In short, we did not find evidence of significant interference or artifacts
429 which would undermine our halogen measurements.

430

431 **Chemical Box Model**

432 An zero-dimensional chemical box model was built based on the latest version of the
433 Master Chemical Mechanism v3.3.1 by using the Kinetic Pre-Processor (KPP) [50] on a
434 MATLAB platform. To better represent the halogen chemistry, we modified the mechanisms
435 to include chlorine and bromine related reactions. The detailed kinetics data adopted in the
436 model are listed in Table S2 and described in the supplementary materials. In this study, we
437 used the model to calculate the impact of Cl and Br atoms on oxidation chemistry. The model
438 was constrained to observations of HONO, O₃, H₂O₂, NO, NO₂, SO₂, CO, temperature, aerosol
439 surface area density, J_{NO₂}, VOCs, and OVOCs. Table S4 shows a summary of the input
440 parameters in the model. Other detailed information on photolysis frequencies, dry deposition,
441 the boundary layer height, the wet deposition is described in the supplementary materials.

442

443

444 **SUPPLEMENTARY MATERIALS**

445 Supplementary materials are available online, which includes:

446 Section S1, CIMS Measurement

447 Section S2, Measurement Site

448 Section S3, Other Measurement Instruments Used in the Work

449 Section S4, Comparison of Ratios of Halogen to Sulfur in Ambient Air and Coals

450 Section S5, Accounting for Observed Halogens

451 Section S6. Chemical Box Model

452 Supplementary Figures: Figure S1 to S14

453 Supplementary Tables: Tables S1 to S4

454 References

455

456 **ACKNOWLEDGMENT**

457 We thank Liwei Guan and Research Center for Eco-Environmental Sciences for providing
458 logistics support. We thank the following persons for their help in field measurements: Chuan
459 Yu (NO_x and O₃), Chaoyang Xue (HONO), Can Ye (H₂O₂), Xiaoxi Zhao (WSI in offline filter),
460 Chongxu Zhang (OVOCs).

461

462 **FUNDING**

463 This work was supported by the National Natural Science Foundation of China (91544213 to
464 T.W., and 21806020 to J.C., and 91544211 and 41727805 to Y.M., and 21976106 to J.W.), and
465 the Hong Kong Research Grants Council (T24-504/17-N and A-PolyU502/16 to T.W.), and
466 the Ministry of Science and Technology of China (2016YFC0202700 to J.C.), and the National
467 research program for key issues in air pollution control (DQGG0103 to J.C. and DQGG0102
468 to H.C.), and the European Research Council Executive Agency under the European Union's
469 Horizon 2020 Research and Innovation programme (Project ERC-2016- COG 726349
470 CLIMAHAL to A.S-L), and the grant SEAM (ANR-16-CE01-0013 to C.G.).

471

472 **AUTHOR CONTRIBUTIONS**

473 T.W. designed halogen research. J.C. and Y.M. planned and organized the overall field
474 campaign at Wangdu. X.P., M.X. and W.W. conducted measurements of the halogen species
475 by CIMS. X.P. and W.W. set up the halogen calibration method, built the chemical box model,
476 and performed laboratory tests. Q.L. helped model development. L.X. helped the box model
477 development and validation. P.L., C.Z. performed measurements of SO₂, NO_x, O₃, HONO, and
478 H₂O₂. H.C., F.Z., C.Z., and J.W. performed VOCs and OVOCs measurements. H.C., P.L., and
479 F.Z. performed particulate matter measurements (elementary analyzer, ACSM, OC, EC, WSI
480 in the offline filter). M.X. and X.W. performed JNO₂ measurements. H.C. and F.Z. performed
481 aerosol size distribution measurements. X.P., W.W., T.W., and A.R.R. analyzed the data and
482 interpreted the results, with contributions from A.S-L, Q.L., C.G., and Y.M.. T.W., X.P., and
483 W.W. wrote the paper, with significant input from A.R.R., A.S-L., and H.C. All authors
484 reviewed and commented on the paper.

485

486 **COMPETING INTERESTS DECLARATION**

487 None declared.

488

489

490 **DATA AVAILABILITY**

491 All data needed to evaluate the conclusions in the paper are present in the paper and/or the
492 Supplementary Materials. CIMS measurement data is available by contacting the
493 corresponding author (T.W.) (cetwang@polyu.edu.hk). Other data is available by contacting
494 J.C. (jmchen@fudan.edu.cn) and Y.M. (yjmu@rcees.ac.cn).

495

REFERENCES

1. Molina, MJ, Rowland, FS. Stratospheric sink for chlorofluoromethanes: chlorine atom-catalysed destruction of ozone. *Nature*. 1974; **249**(5460): 810.
2. Foster, KL, Plastringe, RA, Bottenheim, JW, *et al.* The role of Br₂ and BrCl in surface ozone destruction at polar sunrise. *Science*. 2001; **291**(5503): 471-4.
3. Liao, J, Huey, LG, Liu, Z, *et al.* High levels of molecular chlorine in the Arctic atmosphere. *Nature Geoscience*. 2014; **7**(2): 91.
4. Wang, S, McNamara, SM, Moore, CW, *et al.* Direct detection of atmospheric atomic bromine leading to mercury and ozone depletion. *Proceedings of the National Academy of Sciences*. 2019; **116**(29): 14479.
5. Simpson, WR, Brown, SS, Saiz-Lopez, A, *et al.* Tropospheric halogen chemistry: sources, cycling, and impacts. *Chemical Reviews*. 2015; **115**(10): 4035-62.
6. Obrist, D, Tas, E, Peleg, M, *et al.* Bromine-induced oxidation of mercury in the mid-latitude atmosphere. *Nature Geoscience*. 2010; **4**(1): 22.
7. Hossaini, R, Chipperfield, MP, Saiz-Lopez, A, *et al.* A global model of tropospheric chlorine chemistry: Organic versus inorganic sources and impact on methane oxidation. *Journal of Geophysical Research: Atmospheres*. 2016; **121**(23): 14,271-14,97.
8. Thornton, JA, Kercher, JP, Riedel, TP, *et al.* A large atomic chlorine source inferred from mid-continental reactive nitrogen chemistry. *Nature*. 2010; **464**(7286): 271.
9. Fu, X, Wang, T, Wang, S, *et al.* Anthropogenic emissions of hydrogen chloride and fine particulate chloride in China. *Environmental science & technology*. 2018; **52**(3): 1644-54.
10. Riedel, TP, Wagner, NL, Dube, WP, *et al.* Chlorine activation within urban or power plant plumes: Vertically resolved ClNO₂ and Cl₂ measurements from a tall tower in a polluted continental setting. *J Geophys Res-Atmos*. 2013; **118**(15): 8702-15.
11. McDuffie, EE, Fibiger, DL, Dubé, WP, *et al.* ClNO₂ Yields From Aircraft Measurements During the 2015 WINTER Campaign and Critical Evaluation of the Current Parameterization. *Journal of Geophysical Research: Atmospheres*. 2018; **123**(22): 12,994-13,015.
12. Priestley, M, le Breton, M, Bannan, TJ, *et al.* Observations of organic and inorganic chlorinated compounds and their contribution to chlorine radical concentrations in an urban environment in northern Europe during the wintertime. *Atmospheric Chemistry and Physics*. 2018; **18**(18): 13481-93.
13. Haskins, JD, Lopez-Hilfiker, FD, Lee, BH, *et al.* Anthropogenic Control Over Wintertime Oxidation of Atmospheric Pollutants. *Geophysical Research Letters*. 2019; **46**(24): 14826-35.
14. Tham, YJ, Wang, Z, Li, Q, *et al.* Significant concentrations of nitryl chloride sustained in the morning: investigations of the causes and impacts on ozone production in a polluted region of northern China. *Atmospheric Chemistry and Physics*. 2016; **16**(23): 14959-77.
15. Wang, T, Tham, YJ, Xue, L, *et al.* Observations of nitryl chloride and modeling its source and effect on ozone in the planetary boundary layer of southern China. *Journal of Geophysical Research: Atmospheres*. 2016; **121**(5): 2476-89.
16. Liu, X, Qu, H, Huey, LG, *et al.* High levels of daytime molecular chlorine and nitryl chloride at a rural site on the North China Plain. *Environmental science & technology*. 2017; **51**(17): 9588.

- 540 17. Xue, C, Ye, C, Ma, Z, *et al.* Development of stripping coil-ion chromatograph method
541 and intercomparison with CEAS and LOPAP to measure atmospheric HONO. *Science of The*
542 *Total Environment*. 2019; **646**: 187-95.
- 543 18. An, Z, Huang, R-J, Zhang, R, *et al.* Severe haze in northern China: A synergy of
544 anthropogenic emissions and atmospheric processes. *Proceedings of the National Academy of*
545 *Sciences*. 2019; **116**(18): 8657-66.
- 546 19. Fu, X, Wang, T, Gao, J, *et al.* Persistent Heavy Winter Nitrate Pollution Driven by
547 Increased Photochemical Oxidants in Northern China. *Environmental Science & Technology*.
548 2020; **54**(7): 3881-9.
- 549 20. Lee, BH, Lopez-Hilfiker, FD, Schroder, J, *et al.* Airborne observations of reactive
550 inorganic chlorine and bromine species in the exhaust of coal-fired power plants. *Journal of*
551 *Geophysical Research: Atmospheres*. 2018; **123**.
- 552 21. Liao, J, Huey, LG, Tanner, DJ, *et al.* Observations of inorganic bromine (HOBr, BrO,
553 and Br₂) speciation at Barrow, Alaska, in spring 2009. *Journal of Geophysical Research:*
554 *Atmospheres*. 2012; **117**(D14).
- 555 22. Ren, D, Zhao, F, Wang, Y, *et al.* Distributions of minor and trace elements in Chinese
556 coals. *International Journal of Coal Geology*. 1999; **40**(2): 109-18.
- 557 23. Peng, B-x. Study on Environmental Geochemistry of Bromine in Chinese Coals *Ph.D.*
558 *thesis*. Nanchang University; 2011.
- 559 24. Tang, Y, He, X, Cheng, A, *et al.* Occurrence and sedimentary control of sulfur in coals of
560 China. *Journal of China Coal Society*. 2015; **40**(9): 1976-87.
- 561 25. Du, Q, Zhang, C, Mu, Y, *et al.* An important missing source of atmospheric carbonyl
562 sulfide: Domestic coal combustion. *Geophysical Research Letters*. 2016; **43**(16): 8720-7.
- 563 26. Fan, S-M, Jacob, DJ. Surface ozone depletion in Arctic spring sustained by bromine
564 reactions on aerosols. *Nature*. 1992; **359**(6395): 522-4.
- 565 27. Wennberg, P. Bromine explosion. *Nature*. 1999; **397**(6717): 299-301.
- 566 28. Abbatt, J, Oldridge, N, Symington, A, *et al.* Release of Gas-Phase Halogens by
567 Photolytic Generation of OH in Frozen Halide–Nitrate Solutions: An Active Halogen
568 Formation Mechanism? *The Journal of Physical Chemistry A*. 2010; **114**(23): 6527-33.
- 569 29. Richards, NK, Wingen, LM, Callahan, KM, *et al.* Nitrate Ion Photolysis in Thin Water
570 Films in the Presence of Bromide Ions. *The Journal of Physical Chemistry A*. 2011; **115**(23):
571 5810-21.
- 572 30. Wren, SN, Donaldson, DJ, Abbatt, JPD. Photochemical chlorine and bromine activation
573 from artificial saline snow. *Atmospheric Chemistry and Physics*. 2013; **13**(19): 9789-800.
- 574 31. Pratt, KA, Custard, KD, Shepson, PB, *et al.* Photochemical production of molecular
575 bromine in Arctic surface snowpacks. *Nature Geoscience*. 2013; **6**: 351.
- 576 32. Corral Arroyo, P, Aellig, R, Alpert, PA, *et al.* Halogen activation and radical cycling
577 initiated by imidazole-2-carboxaldehyde photochemistry. *Atmospheric Chemistry and*
578 *Physics*. 2019; **19**(16): 10817-28.
- 579 33. Wang, X, Jacob, DJ, Eastham, SD, *et al.* The role of chlorine in global tropospheric
580 chemistry. *Atmospheric Chemistry and Physics*. 2019; **19**(6): 3981-4003.
- 581 34. Hoffmann, EH, Tilgner, A, Wolke, R, *et al.* Enhanced Chlorine and Bromine Atom
582 Activation by Hydrolysis of Halogen Nitrates from Marine Aerosols at Polluted Coastal
583 Areas. *Environmental Science & Technology*. 2019; **53**(2): 771-8.

- 584 35. Tan, Z, Rohrer, F, Lu, K, *et al.* Wintertime photochemistry in Beijing: observations of
585 ROx radical concentrations in the North China Plain during the BEST-ONE campaign.
586 *Atmospheric Chemistry and Physics*. 2018; **18**(16): 12391-411.
- 587 36. Saiz-Lopez, A, Sitkiewicz, SP, Roca-Sanjuán, D, *et al.* Photoreduction of gaseous
588 oxidized mercury changes global atmospheric mercury speciation, transport and deposition.
589 *Nature Communications*. 2018; **9**(1): 4796.
- 590 37. Wang, Q, Shen, W, Ma, Z. Estimation of mercury emission from coal combustion in
591 China. *Environmental Science & Technology*. 2000; **34**(13): 2711-3.
- 592 38. NRDC. *China 13th Five-Year Plan (2016-2020) Coal Consumption Cap Plan and*
593 *Research Report*. Natural Resources Defense Council; 2016,
594 <http://nrdc.cn/Public/uploads/2017-01-12/5877316351a6b.pdf>.
- 595 39. NDRC. Clean winter heating plan for Northern China (2017-2021) (in Chinese). The
596 National Development and Reform Commission of China; 2017.
- 597 40. CAA. *Winter Residential Heating in Typical Rural Northern China Report (in Chinese)*.
598 Clean Air Asia; 2019, <http://www.allaboutair.cn/a/reports/2019/1031/564.html>.
- 599 41. National Joint Research Center for Tackling Key Problems in Air Pollution Control: It's
600 a tough and protracted battle (in Chinese), Available at:
601 http://www.mee.gov.cn/ywgz/dqjhjbh/dqhzjzlg/202002/t20200214_764011.shtml,
602 (Accessed:2020, Feb 10).
- 603 42. Liu, J, Mauzerall, DL, Chen, Q, *et al.* Air pollutant emissions from Chinese households:
604 A major and underappreciated ambient pollution source. *Proceedings of the National*
605 *Academy of Sciences*. 2016; **113**(28): 7756-61.
- 606 43. Barrington-Leigh, C, Baumgartner, J, Carter, E, *et al.* An evaluation of air quality, home
607 heating and well-being under Beijing's programme to eliminate household coal use. *Nature*
608 *Energy*. 2019; **4**(5): 416-23.
- 609 44. IEA. *International Energy Agency World Energy Statistics, 1960-2018*. International
610 Energy Agency; 2020, <http://doi.org/10.5257/iea/wes/2019>.
- 611 45. Yang, X, Wang, T, Xia, M, *et al.* Abundance and origin of fine particulate chloride in
612 continental China. *Science of The Total Environment*. 2018; **624**: 1041-51.
- 613 46. Wang, Z, Wang, W, Tham, YJ, *et al.* Fast heterogeneous N₂O₅ uptake and ClNO₂
614 production in power plant and industrial plumes observed in the nocturnal residual layer over
615 the North China Plain. *Atmospheric Chemistry and Physics*. 2017; **17**(20): 12361-78.
- 616 47. Buys, Z, Brough, N, Huey, LG, *et al.* High temporal resolution Br₂, BrCl and BrO
617 observations in coastal Antarctica. *Atmospheric Chemistry and Physics*. 2013; **13**(3): 1329.
- 618 48. Neuman, JA, Nowak, JB, Huey, LG, *et al.* Bromine measurements in ozone depleted air
619 over the Arctic Ocean. *Atmospheric Chemistry and Physics*. 2010; **10**(14): 6503-14.
- 620 49. Le Breton, M, Bannan, TJ, Shallcross, DE, *et al.* Enhanced ozone loss by active
621 inorganic bromine chemistry in the tropical troposphere. *Atmospheric Environment*. 2017;
622 **155**: 21-8.
- 623 50. Sandu, A, Sander, R. Technical note: Simulating chemical systems in Fortran90 and
624 Matlab with the Kinetic PreProcessor KPP-2.1. *Atmospheric Chemistry and Physics*. 2006;
625 **6**(1): 187-95.